Proceedings of the ASME 2009 28th International Conference on Ocean, Offshore and Arctic Engineering
OMAE2009
May 31 - June 5, 2009, Honolulu, Hawaii, USA

OMAE2009-79793

MEASUREMENT OF THE EFFECT OF POWER ABSORPTION IN THE LEE OF A WAVE ENERGY CONVERTER

Ian G. C. Ashton[1]
I.G.C.Ashton@exeter.ac.uk

Lars Johanning[1]
L.Johanning@exeter.ac.uk

Brian Linfoot[2]
B.T.Linfoot@sbe.hw.ac.uk

[1.] School of Geography, Archaeology and Earth Resources,
University of Exeter, Cornwall Campus TR10 9EZ, UK

[2.] School of the Built Environment, Sir William Arrol Bldg.,
Heriot-Watt University, Edinburgh, EH14 4AS, UK

ABSTRACT

Monitoring the effect of floating wave energy converter (WEC) devices on the surrounding wave field will be an important tool for monitoring impacts on the local wave climate and coastlines. Measurement will be hampered by the natural variability of ocean waves and the complex response of WEC devices, causing temporal and spatial variability in the effects. Measurements taken during wave tank tests at MARINTEK are used to analyse the effectiveness of point wave measurements at resolving the influence of an array of WEC on the local wave conditions. The variability of waves is measured in front and in the lee of a device, using spectral analysis to identify changes to the incident wave field due to the operating WEC. The power capture and radiation damping are analysed in order to predict the measured changes. Differences in the wave field across the device are clearly observable in the frequency domain. However, they do not unanimously show a reduction in wave energy in the lee of a device and are not well predicted by measured power capture.

Keywords: wave energy, wave energy impacts, wave measurements, wave tank testing

1. INTRODUCTION

Experiences in the planning phase of the Wave Hub development, Cornwall, UK, highlighted stakeholder concern about the potential effects of wave energy developments through changes in the wave climate at the coastline [1]. As wave energy companies move towards commercial deployment, many leading designs involve multiple devices deployed in arrays, which have the potential to remove significant energy from the wave climate on site.

The change in wave climate in the lee of a development will depend on the response of devices to the incident wave field. Modelling of downstream impacts has been attempted. However, predicting the response of a WEC to the incident waves commonly involves simplification of the physical properties of the device and the incident wave field. Examples include [2], who represented WECs as a bottom-mounted structure with varying porosity levels. A similar approach using partially transmitting barriers to represent wave farms was also attempted in the literature [3, 4]. A more accurate representation of operating devices must take into account the dependence of their response on incident wave field properties, such as frequency, amplitude, spectral shape and direction. However, as an emerging technology, there is very little operational data available to validate modelling and predictions for WECs in real sea conditions, and none that concerns arrays.

Robust measurements of the change in wave energy as waves pass through a wave farm would capture variability in the effect, enable validation of array-scale hydrodynamic modelling, and serve as inputs for predictive modelling of the

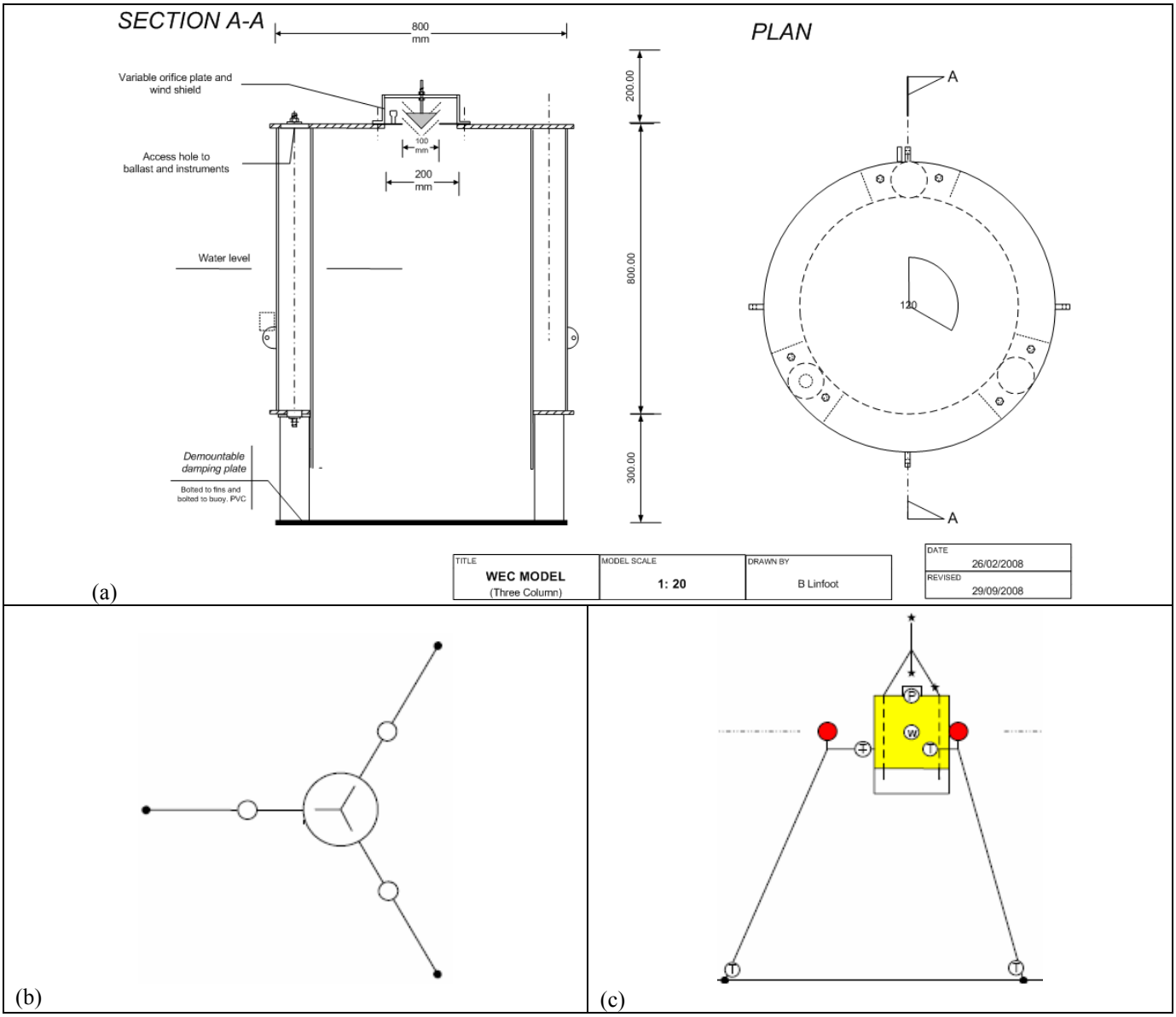

Figure 1a-c. SCHEMATIC OF WEC DEVICE MODEL

effect on the wave climate at the coastline. Furthermore, stakeholders have called for a program of monitoring of early developments [5]. Measurement regimes are planned using conventional wave measurement technology, such as wavebuoys or ADCP's, which measure the wave conditions in front, and in the lee of operating devices [6]. A number of challenges that must be overcome in deriving robust measurements of a wave farms impact using such methods have been identified, such as:

- High variability of the properties of the incident wave field and associated variations in device response, mean that a significant data set will be required in order to relate measurements to wave conditions.
- Random variations inherent in processing and describing a random wave field will introduce variability in measurements taken around a development, and may mask the impact of WEC devices.
- The response of devices and complex interactions within the array will mean that changes in the lee of the devices are likely to exhibit spatial patterns that will not be well resolved by point measurements.

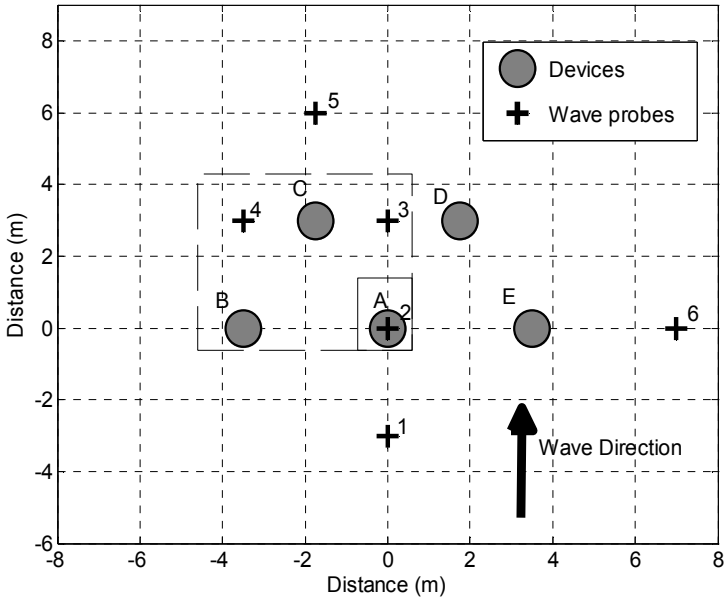

Figure 2. WAVE TANK SET-UP. BOXES SHOW THE DEVICES USED IN EACH TEST.

In this paper, scale wave tank tests are used in a preliminary analysis into the effectiveness of point measurements at resolving the influence of WECs on the propagating wave field. Wave measurements are compared to the magnitude of power absorbed and the radiated waves, in order to qualify observed changes to the wave field. Understanding the influence of devices on the surrounding wave field will be key to developing effective monitoring regimes and interpreting results from wave measurement devices around a wave energy development.

2. EXPERIMENT DESIGN

The tests were conducted at 1:20 scale in the MARINTEK wave tank, Trondheim. The wave tank is 2.8m deep, 80 metres wide and 50 metres long with a beach on two sides and wave makers on the opposite sides. Tests were performed in a range of regular (monochromatic) and irregular sea-states, generated from a Bretschneider spectrum. Initial calibration was performed without devices and subsequently the tests were repeated for 1 device (A), and arrays of 3 (A,B &C) and 5 devices. The model devices represent a generic oscillating water column (OWC) type device. They were designed as cylindrical bodies (Fig. 1a) and moored using a three leg mooring arrangement (Fig. 1b). The configuration of a mooring leg consisted of a fibre rope from the anchor to a surface buoy which was linked via a second rope to fairlead at the WEC (Fig. 1c). The power take off system (PTO) was represented by a small orifice in the top of the buoy, whose size was calibrated to offer the maximum absorption of incident power. All figures used in the following will refer to the full-scale and therefore have been accordingly scaled from the raw data.

During the tests a total of six wave probes were situated around the array, measuring water surface elevation. As a result of time restraints, for the preliminary analysis presented here wave data from probes 1 and 3, situated in front and in the lee of device A (Fig. 3), are used. These two probes offer direct measurement of the change in wave conditions as the waves propagate through the device. This is also compared to data from probe 5. The measurement package installed on the devices included a motion tracking system, providing motion in 6 degrees of freedom as well as in-line load cells and inclination instrumentation at the fairlead. Data were sampled at 80Hz which relates to a scaled rate of 17.89Hz

3. WAVE CALIBRATION

Calibration tests were performed without any WECs installed to identify variability and repeatability of the wave conditions. This was required in order to quantify the variability associated with the physical properties of the tank to inform estimations of the influence of the devices.

Table 1. MEASURED VALUES FOR THE RMS DERIVED WAVE AMPLITUDE FOR MONOCHROMATIC WAVES.

Input wave height (m)	RMS wave heights at probe: 1	3	5	6
1	1.17	1.36	1.16	1.16
1	1.03	1.20	1.09	1.11
1	0.89	0.95	1.24	0.96
1	1.19	1.35	1.07	1.42
1	0.89	1.19	1.31	1.09
1	1.45	0.91	0.96	0.91
1.5	1.31	1.50	1.83	1.72
2	1.95	1.77	2.25	2.12
2.5	2.47	2.02	2.91	2.55
3	2.90	2.51	3.54	3.09

Analysis of the monochromatic test data showed that there is significant variability in the wave conditions at different positions around the tank, possibly caused by wave reflection. This contributed to high variation in the root mean square (RMS) wave amplitudes (Tab. 1). Therefore, the variation in the wave conditions due to the presence of the WECs cannot be accurately measured because wave tank variations themselves dominate observed conditions. In this analysis, no suitable method could be identified to eliminate the tank effect and hence monochromatic waves were not further investigated.

Calibration tests conducted for irregular wave states generated to a Bretschneider spectrum, showed less variability and matched the input wave conditions more closely. Repetition of calibration tests found the wave spectra to be closely matched for repeat tests (Fig. 3a) and significant wave height and total power to vary by less than 1% (Tab. 2). Examination of the time series for repeated tests using irregular waves show that the exact form of the waves generated is also closely

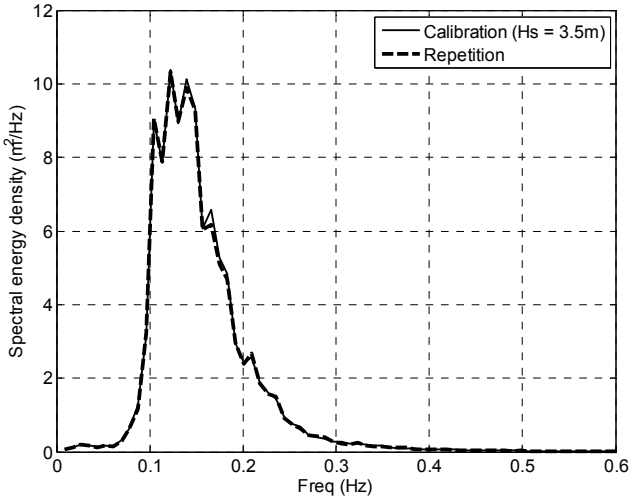

(a)

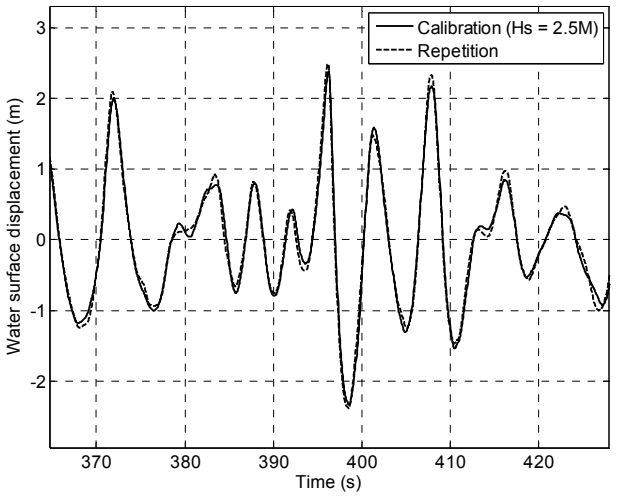

(b)

Figure 3. (a) WAVE SPECTRA AND (b) TIME SERIES FOR REPETITION TEST DURING CALIBRATION

matched between repeats (Fig. 3b). Therefore, changes observed during irregular wave tests can be attributed to the presence of the devices.

4. WAVE RADIATION EFFECTS

Oscillating structures radiate waves to the surrounding fluid, which must be considered when analysing the wave field around operating devices. Decay tests in still water were conducted for heave, pitch and surge motions with the moorings attached. During the tests the device was displaced, before the restraint was removed allowing a free transient motion. The resultant time history for the heave motion test is shown in Fig. 4a. The motion characteristics were analysed in terms of amplitude, period and damping characteristics (Tab. 3). This

Table 2. SIGNIFICANT WAVE HEIGHTS MEASURED DURING CALIBRATION TESTS FOR IRREGULAR WAVES.

Input wave height (m)	H_{m0} (m) at probe: 1	3	5	6
2.5	2.84	2.90	2.90	2.86
3.5	3.81	3.87	3.90	3.81
3.5 repeat	3.79	3.86	3.86	3.83

motion can be matched to the far field radiated waves. During these tests, wave probes measured the time-series of the radiated wave field around the devices (Fig. 4b). Analysis of all three modes identified that in all cases the dominant frequency of the radiated waves matched that of the heave motion. The likely cause of this is that inadvertent vertical pressure was applied during the manual displacement of the device during pitch and surge tests. As a consequence, heave motions were dominant and the radiated waves measured during the other decay tests were not analysed further.

The average period of the waves measured during the heave decay test was eight seconds, which closely matches the natural heave frequency of the device and mooring system (Tab. 3). The wave amplitude was analysed and related to the transient heave motion of the device. From this, the ratio of wave amplitude to device motion was calculated as $a_w/\eta = 0.22$. Using this ratio, the amplitude of the expected radiated waves during the tests can be estimated. Furthermore, an estimation of the wave radiation and damping can be made using theoretical methods, where the damping has a contribution to the power capture and motion response.

Table 3. NATURAL PERIOD, LOGARITHMIC DECREMENT, Λ, AND TOTAL DAMPING, ξ_{tot}, CALCULATED DURING STILL WATER TESTS.

	Natural Period	Λ	ξ_{tot}
Pitch	19.4	0.48	0.025
Heave	7.8	0.36	0.045
Surge	283.9	0.76	0.003

4.1 Theoretical Estimations Of Radiation Damping

Forces acting on a floating body can be considered as a combination of external forces and added mass, damping and restoring forces. In order to calculate the latter group a forced oscillation of the body in still water is considered. Waves will be created by the motion and will propagate away from the device. The oscillatory motion will cause pressure variations across the body. Integrating over the whole surface gives the resultant forces on the body. Defining these forces in *x,y,z* directions gives [7]

$$F_k = A_{kj}\frac{d^2\eta}{dt^2} + B_{kj}\frac{d\eta}{dt} \quad (1)$$

Where A represents added mass with the acceleration $\frac{d^2\eta}{dt^2}$ and B represents the total damping with the velocity $\frac{d\eta}{dt}$. The subscription k relates to the six directions of forcing, while j relates to the body response in all modes of motion for a floating body.

A floating oscillating body can be considered as a classic spring-mass-damping system. Total damping is the sum of structural and hydrodynamic damping. Hydrodynamic damping comprises both viscous and wave radiation damping, whilst structural damping will include the power capture. As a body oscillates freely in the absence of forcing, the total damping can be identified by the transient peak displacement over N cycles

$$\xi_0 + \xi_w + \xi_v = \ln\left(\frac{x(t)}{x(t+TN)}\right)/N, \quad (2)$$

where ξ_0 is the structural damping, ξ_w is the radiation damping and ξ_v is the viscous damping.

Total damping in pitch, heave and surge motions were found during decay tests and are given in Tab. 3.

For a body oscillating in still water, energy dissipated due to the radiation damping is equivalent to the energy in the radiated waves. Therefore, the energy contained in one cycle of the generated wave gives the damping factor due to wave radiation. It follows that conventional estimations of radiation damping can be applied here to estimate the magnitude of the radiated wave. Treating the device as a surface piercing floating cylinder, methods have been developed and implemented in order to solve analytically for the radiated waves from the body for different motions. An equation for the radiation damping force per unit velocity and length in heave motion was derived in the form [7]

$$B_{33} = \rho\left(\frac{a_w}{|\eta_3|}\right)^2\frac{g^2}{\omega^3}, \quad (3)$$

where a_w is the amplitude of the radiated wave and $|\eta_3|$ is the amplitude of the heave motion. Substituting the measured ratio, $a_w/\eta = 0.22$, into this equation allows estimation of the radiation damping force per unit velocity and length, associated with the heave motions of the device. Incorporating the mass of the device into equation (3), critical damping associated with wave radiation can be calculated. However, the critical damping, as shown in Tab. 3., represents the total damping and hence a direct comparison is not possible. Nevertheless, the calculated damping from (3) results in a value of $\xi_{tot} = 0.052s^{-1}$, which is close to the measured value (Tab. 3).

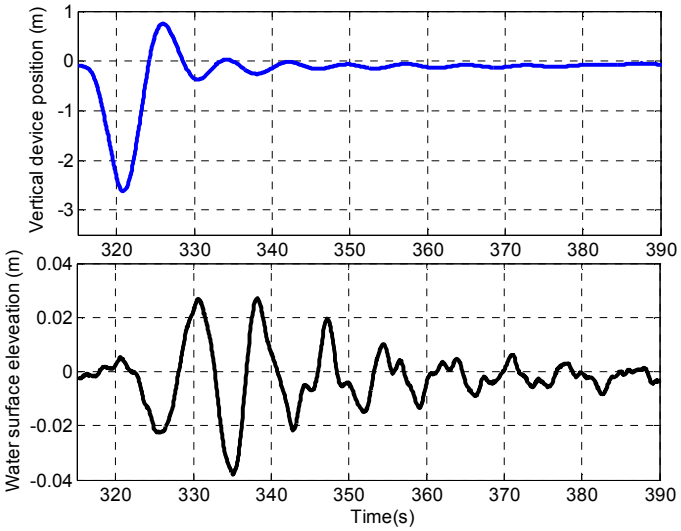

Figure 4. HEAVE MOTION DURING DECAY TEST FOR (a) DEVICE AND (b) RADIATED WAVES

In order to predict the wave radiation damping in pitch and surge, theoretical methods can be applied. Radiation damping for pitch and surge modes was estimated using a frequency domain solution described in [8]. Here an approach is applied based on wave maker theory [9], described in [10] for sway and in [11] for pitch motion.

In planar motion, the energy input from a cylinder becomes

$$E = \frac{|A_0|^2(\sinh(kh)+2kh)}{2k}2\pi\rho \quad (4)$$

Where h is the water depth. For a sway (or equivalently surge) motion, the co-efficient |A0| becomes

$$A_0\frac{2\omega\hat{x}_{11}\sinh(k_0h)e^{-iv}}{\sinh(2k_0h)+2k_0h}\frac{1}{(ak_0)[H_1^{(1)}(k_0a)]'} \quad (5)$$

where a is the radius of the cylinder, $v = \tan^{-1}(Y_1(k_0a)'/J_1(k_0a)')$ is the phase angle and $H_1^{(1)}(k_0a)$ is the Hankel function of the first kind where $Y_1(k_0a)$ and $J_1(k_0a)$ are Bessel functions. Equating the energy required to generate waves to the dissipated energy over one cycle, gives

$$\xi_w = \frac{4\rho a^3(\sinh(k_0h))^2}{M\lambda(\sinh(2k_0h)+2k_0h)}\frac{(e^{-iv})^2(H(k_0a))^2}{k_0a} \quad (6)$$

where

$$H(k_0a) = \{(k_0a)[H_1^{(1)}(k_0a)]\}^{-1} \quad (7)$$

A similar formulation applied to pitch mode gives

$$\xi_w = \frac{\rho D^2}{M}\frac{a}{d}\frac{1}{ka(kh)^2}\Psi_{wr} \quad (8)$$

where d is the draught, D is diameter and M the mass of the cylinder, and

$$\Psi_{wr} = \frac{(kh\sinh(kh) - \cosh(kh) + 1)^2}{\sinh(2kh) + 2kh}(H(ka))^2 e^{-2iv} \quad (9)$$

Figure 5 shows the theoretically predicted radiation damping for both pitch and surge modes, where *ka* is the wave number of the radiated waves multiplied by the radius of the cylinder. Also marked are the values for total damping as calculated from the transient pitch and surge motion tests (Tab. 3). In both cases, the theoretical predictions of radiation damping are less than the measured values for total damping, as expected.

From the above estimations of radiation damping, it can be predicted that the surge wave radiation will have a minimum effect in comparison to pitch and heave. However, the theoretical radiation curve predicts that oscillations at the natural frequency in pitch will be in the higher range for radiation damping. Therefore, the resultant radiated waves may have an influence on the wave field analysis.

5. POWER CAPTURE

For a WEC, power take off systems will remove energy from the propagating waves and cause a reduction in wave power in its lee. In order to identify whether a measured reduction in wave power can be attributed to power absorbed by the device, it is necessary to establish robust estimates of the power capture. For an OWC, incident waves will cause varying water surface height within the device. The resultant pressure fluctuations in the trapped air column force air through a turbine. Power capture is therefore dependant on the internal pressure and the volume flux. For these tests, the turbine is simulated by a controlled orifice at the top of the device (Fig. 1a).

The instrumentation included wave probes measuring the internal water level within the devices and pressure gauge near the orifice. Assuming that the water retains a planar surface and that the surface angle, relative to the walls is always close to 90°, this allows estimation of the change in volume of the air column within the device, ΔV . The measured pressure, *p,* in the internal air chamber was then used to calculate the power capture in the form

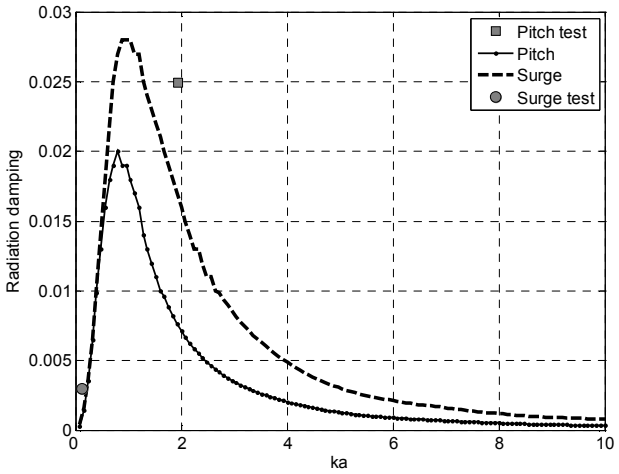

Figure 5. THEORETICAL ESTIMATED RADIATION DAMPING FOR DEVICES UNDER A RANGE OF WAVENUMBERS, (d = 0.147h, AND a/h = 0.107)

$$P_{ave} = \frac{1}{n\Delta t}\sum_{i=1}^{i=n} p(t_i)\Delta V(t_i), \quad (10)$$

where *n* is the number of data points in the record and Δt is the time step. The power capture by device A during tests with 1, 3 and 5 installed devices is shown in Tab. 4. The power calculated here represents the average power absorbed by the device, P_{ave}, which measures 16m in diameter. For further comparison, the power absorbed per metre, *P,* was also calculated and is also shown in Tab. 4.

The calculated power capture shows that the device, A is absorbing power from the propagating wave field in all tests Small variations between the tests with 1,3 and 5 devices installed can be observed. However, at this stage no conclusion can be made as to their cause.

Table 4. THE AVERAGE POWER CAPTURE, CALCULATED USING (10)

N° of WECs installed during test	P_{ave} (kW)	P (kW/m)
1	96.47	6.03
3	95.73	5.98
5	101.5	6.34

6. WAVE MEASUREMENTS

During the tests, the wave field was measured at wave probes situated before and after device A (Fig. 2). The situation of these wave probes allows measurements of the difference in the wave power before and in the lee, for the single installation of device A. The arrangement of 3 and 5 WEC array installations also shows the influence of surrounding devices on this difference. The difference in measured wave power is

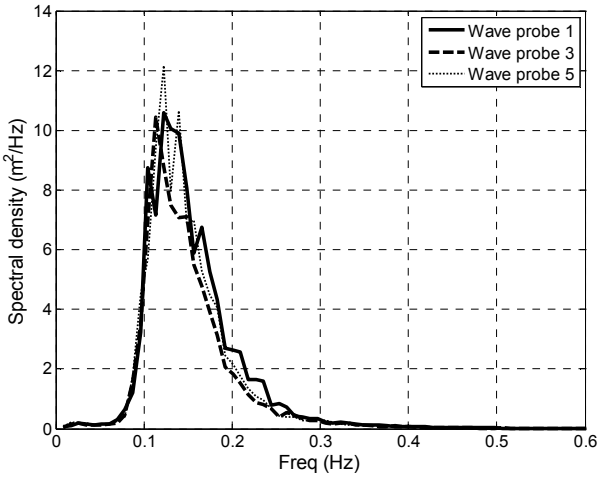

(a)

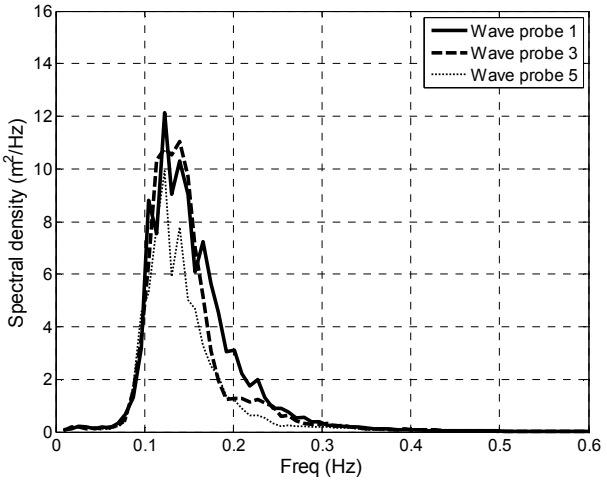

(b)

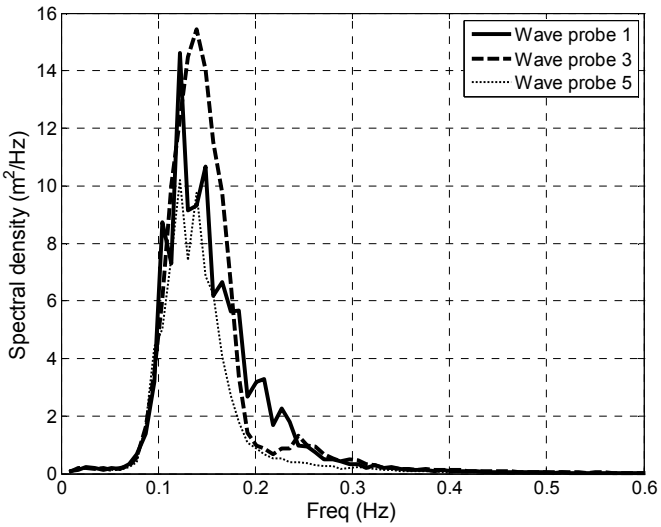

(c)

Figure 6. WAVE SPECTRA FOR UPSTREAM WAVE PROBE 1, DOWNSTREAM WAVE PROBE 3 AND WAVE PROBE 5. FIGURE (a) PRESENTS WEC A INSTALLED, (b) WEC A-C INSTALLED, (c) WEC A-E INSTALLED.

calculated and compared to the power capture by device A during all three tests.

The measured wave field at each wave probe was spectrally analysed to give a one-dimensional wave spectrum. From this, the wave energy was calculated using

$$E = \rho g(m_0), \tag{11}$$

where $m_0 = \int S(f)df$ and $S(f)$ represents the estimated wave spectrum. The power can be calculated according to the group speed of the waves

$$P = \rho g m_0 c_g, \tag{12}$$

where in finite water depth, c_g can be calculated as

$$c_g = \frac{1}{2}\left[1 + \frac{2kh}{\sinh(2kh)}\right]\frac{gT}{2\pi}\tanh(kh). \tag{13}$$

Thus, from the spectral analysis of the wave field, the incident wave power can be calculated for each wave probe.

Wave spectra from wave probes 1, 3 and 5 are plotted for all tests (Fig. 6a-c). The difference between the plots on each graph indicates the difference in power in front and from two locations in the lee of the devices. As such, these graphs show the frequencies at which the devices affect the wave field.

In Fig 6a., only device A is in place. Here, a reduction in wave power can be seen at wave probe 3, directly in the lee of device A. This is manifest as a decrease in spectral density across the majority of the active spectrum, with the exception of the lowest frequencies. Measurements from the same positions

but with three devices in place show that at the peak frequencies, the power reduction observed at wave 3 is less (Fig. 6b). Through comparing Fig 6a and 6b, it can be observed that the wave spectrum both at probe 3 and at probe 1 increase with two more devices installed. For tests when 5 devices are installed, increases in the wave spectra at probe 1 and 3 are again observed. The increase is largest at wave probe 3, principally at frequencies between 0.12 and 0.19Hz (Fig 6c). This leads to wave probe 3 exhibiting the larger spectrum, indicating an increase in wave power in the lee of the device A when all 5 devices are installed. With 3 and 5 devices installed, wave probe 5 is directly in the lee of device C, and the measured wave field is notably reduced. This device does not exhibit an increased wave spectrum with more devices installed.

6.1 Quantifying the power capture from device A, using wave measurements from probes 1 and 3

From the wave spectrum, the difference in measured wave power can be quantified using (12). The incident wave power calculated for tests with 1, 3 and 5 installed devices is shown in Tab. 5. From these values, the proportional difference in power, ΔP_w between probe 1, P_1, in front of the devices, and probe 3, P_3, in the lee can be calculated (Tab. 5). A positive difference means that incident power was reduced in the lee of the device. These differences, shown in Tab. 5, can be compared to the power capture, P, shown in Tab. 4. Figure 7 plots the calculated difference in power from the power capture and the wave probe measurements, for tests with 1, 3 and 5 devices installed.

Table 5. THE INCIDENT WAVE POWER MEASURED AT WAVE PROBES 1 AND 3

N° of WECs during test	P_1 (kW/m)	P_3 Wave (kW/m)	ΔP_w (kW/m)
1	55	45.92	9.08
3	57.7	51.81	5.89
5	60.58	67.44	-6.86

Both for the test with a single device, and that with three devices installed, the measurements in the lee of device A identify a reduction in wave power (Fig. 7). For a single device, the wave probes identify a reduction in wave power of 9.08kW/m, although power capture was calculated as 6.03kW/m. Therefore a greater reduction in wave power was measured in the lee than power absorbed by the WEC. For three installed devices, power difference and captured power matches closely (ΔP_w = 5.89kW/m, P = 5.98kW/m). When all 5 devices are installed, the power capture does not vary considerably from the other tests, (P = 6.34kW/m). However, an increase in the measured wave power in the lee of the device can be seen as a negative value for ΔP_w = -6.86kW/m.

A WEC designed as a floating body will not only absorb waves, it will also interact with the incident waves and influence

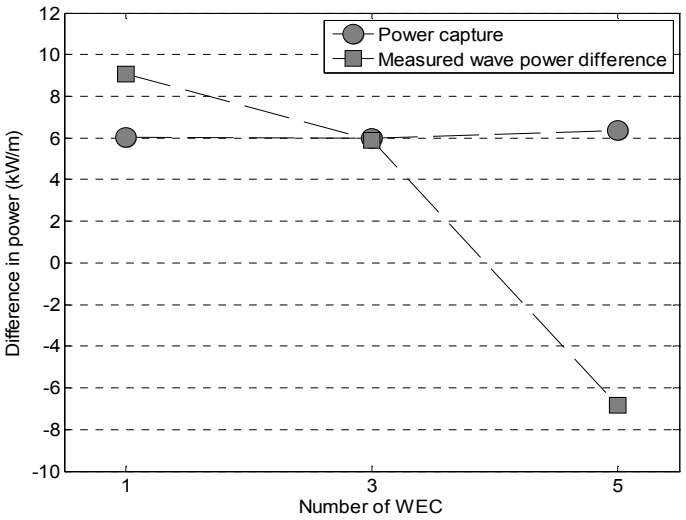

Figure 7. THE POWER CAPTURE CALCULATED FOR DEVICE A, AND THE DIFFERENCE IN MEASURED WAVE POWER BETWEEN PROBE 1 AND 3, AND BETWEEEN 1 AND 5

the surrounding wave field, due to radiation, reflection and diffraction. In the case of this device model, wave absorption is expected to represent the strongest influence on the downstream wave conditions. However it can be seen in Fig 7. that the difference in wave power measured between the probes 1 and 3 does not follow the magnitude of power absorbed by device A. Inspection of the estimated wave spectra at these probes shows that incident wave power measured increases as the number of WEC installed during the test increases (Fig. 6).

Calibration tests, with no devices installed found a difference in incident wave power measured at these wave probes to be less than 1kW/m between repetitions (Fig. 3a). However, when 5 devices are installed, probe 1 shows an increase in incident wave power of 4.5kW/m from the calibration test. This increase is manifest across most of the active frequencies, with the exception of the low frequencies (Fig. 8a).

In the case of wave probe 3 (Fig. 8b), in the lee of device A, a reduction in power of 11.4kW/m from the calibration spectrum is seen for the test with one installed WEC. However, subsequent to this reduction, an increase in the spectral energy occurs for tests where more devices are installed. The wave power incident on wave probe 3 during the test with three installed WECs is 5.49kW/m and for five WECs installed is 10.1kW/m, larger than during the calibration tests.

On-board measurements show that power is being absorbed by device A, however the measurements from wave probes 1 and 3 show a clear effect of the devices to increase the wave fields at these locations. It is assumed that radiation, and to a lesser extent diffraction by the devices are responsible for the greater observed increase at probe 3. Its situation within the array means that it is subject to a complex combined contribution from all devices, which may focus the wave field at this point. In order to quantify the power difference due to device A from wave probes 1 and 3, a full hydrodynamic study of all devices would be required, which is beyond the scope of

this paper. However, the measurements taken during the tests will allow further study in order to examine the interactions within the array and the resultant wave field.

7. CONCLUSIONS

This study represents a preliminary analysis into the variability of wave fields surrounding arrays of devices. Its aim was to analyse how well point wave measurements resolve the downstream impact of an operating WEC on the propagating wave climate. In this initial study, measurements of power capture and theoretical predictions of wave radiation damping have been made in order to analyse the influence of a device on the surrounding wave field. For heave, surge and pitch motions, the radiated waves were estimated using theoretical formulations for radiation damping. These showed that for this system, radiated waves would be principally due to heave and pitch motions and these could be significant in the surrounding wave field. Power capture was calculated using on-board measurements of volume flux and internal air pressure.

Tests were run for the device alone and as part of an array of 3 and 5 WEC. Measurements taken in front of, and in the lee of a single device were analysed in order to identify if a reduction in propagating wave power due to the power capture can be measured. When compared to calculations of power capture, these measurements identify an unexpected increase in the measured wave power when multiple devices are installed, which is largest at probe 3 with 5 devices installed. Wave spectra from an additional probe behind the array were also estimated. These show a reduction in spectral energy when devices are installed, and do not reflect the increase seen at probe 3. In total, six probes were deployed during the tests. All the deployed probes, situated around the array (Fig. 2), will be used in further research into the spatial distribution and propagation of the measured effects.

The measured increase in wave power at wave probe 3 indicates that hydrodynamic effects dominate the power capture in the measured near-field wave states. This was supported through the increase in spectral density with the number of installed devices measured at probe 1 (Fig. 8a). It is therefore not possible to quantify the influence of device A on the propagating wave field by deriving the difference between measurements at probes 1 and 3. Further research is required, including a full hydrodynamic analysis of the body, in order to understand the contribution of complex interactions within the array. This has not been possible within the time constraints on this preliminary analysis and will be subject to continuing work.

At this stage, no clear information can be given whether this form of point wave measurement is suitable to quantify the impact of WEC on the propagating wave field. However, spatial variability around this array has been seen to be significant. These results demonstrate the influence of the placement of point wave sensors on the wave field measured, which must be considered when analysing wave measurements for impact studies. In order to provide a more detailed picture of the wave field, further measurement points are required. Subsequently it

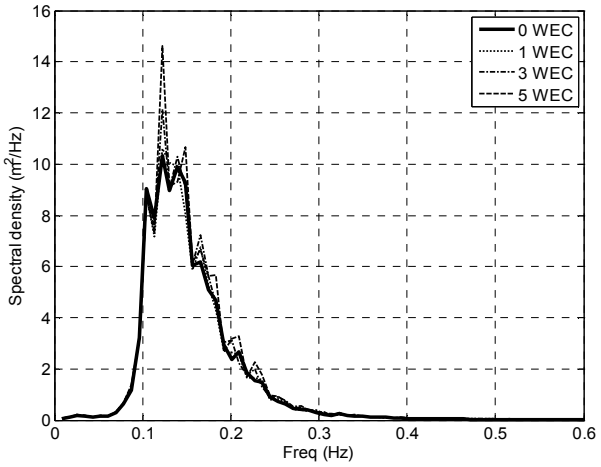

(a)

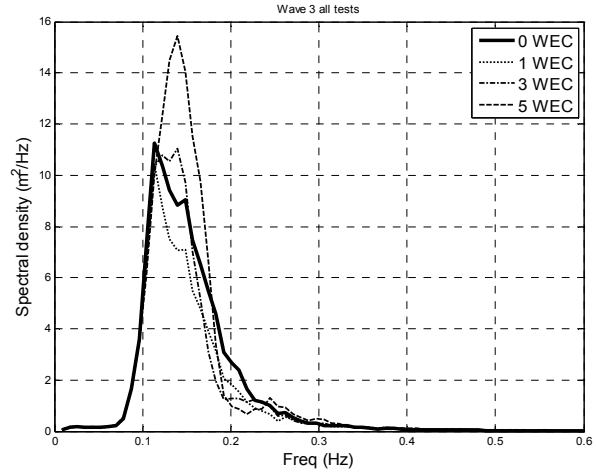

(b)

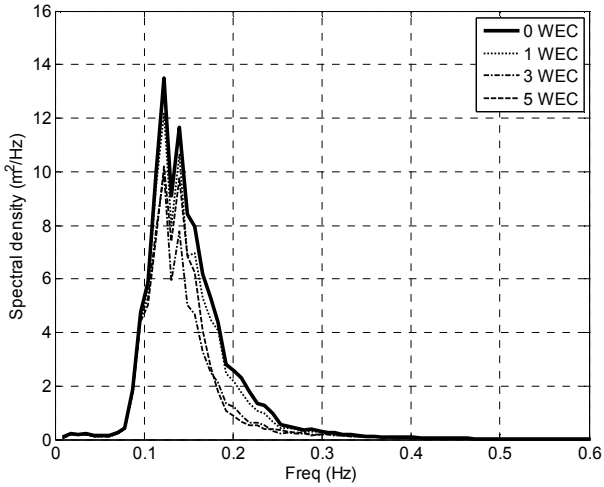

(c)

Figure 8. WAVE SPECTRA FOR EACH TEST AT (a) WAVE 1, INFRONT OF THE DEVICES, (b) WAVE 3, BEHIND DEVICE A, AND (c) WAVE 5, BEHIND DEVICE C

will be important to predict ahead the power capture in conjunction with the hydrodynamic effects, in order to place the wave measurement probes and analyse their output.

The application of wave measurements to practical applications will also require an understanding of how differences measured in the waves on site propagate into the far field, where waves would not be dominated by the local variations due to diffraction and re-radiation. The degree to which one can obtain far-field measurements in a tank is limited by physical constraints, which raises the question of what will constitute the far field and whether this can be obtained at reasonable scale within a tank.

ACKNOWLEDGMENT

The authors would like to acknowledge the Engineering and Physical Science Research Council for its support through the SUPERGEN marine energy research consortium. They also acknowledge the support of the South West Regional Development Agency for its support through the PRIMaRE institution. The work described in this publication was supported by the European Community's Sixth Framework Programme through the grant to the budget of the Integrated Infrastructure Initiative HYDRALAB III, Contract no. 022441 (RII3). The leading author would like to thank his PhD supervisor, Prof. George Smith, for his support.

REFERENCES

[1] Halcrow, 2006. Wave hub non-technical summary. Accessed on-line, June. URL www.wavehub.co.uk.

[2] Venugopal, V., and Smith, G., 2007. “Wave climate investigation for an array of wave power devices”. In Proceedings of the 7th European Wave and Tidal Energy Conference, Porto, Portugal.

[3] Smith, H. C. M., l Millar, D., and Reeve, D. E., 2007. Generalisation of wave farm impact assessment on inshore wave climate”. In Proceedings of the 7th European Wave and Tidal Energy Conference, Porto, Portugal, CSM.

[4] Le Crom, I., Brito-Melo, A., and Sarmento, A., 2008. “Maritime Portuguese pilot zone: analysis of the impact on surfing conditions”. In Proceedings of the 2nd international conference on ocean energy, Brest, France.

[5] Black, K., 2007. Review of wave hub technical studies: Impacts on nearshore surfing beaches. Review, ASR Ltd, Marine Consulting and Research, 7 Wainui Rd, Raglan, NZ.

[6] Smith, G, H., Ashton, I, G, C., and Evans, M, J., “Spatial variation of wave parameters at site specific scale”. In Proceedings of the 2nd international conference on ocean energy, Brest, France.

[7] Faltinsen, O., 1990. Sea loads on ships and offshore structures. Cambridge University Press.

[8] Yeung, R, W., 1981. “Added mass and damping of a vertical cylinder in finite-depth waters.” Applied Ocean Research 3, July, pp. 119-133.

[9] Dean, R., and Dalrymple, R., 1984. Water wave mechanics for engineers and scientists. Prentice Hall.

[10] Johanning, L., Bearman, P. W., and Graham, J. M. R., 2001. “Hydrodynamic damping of a large scale surface piercing circular cylinder in planar oscillatory motion”. Journal of fluids and structures, 15, pp. 891–908.

[11] Johanning, L., 2008. “Dynamic response characteristics of a floating wind turbine tower at low response frequency” No. OMAE2009-79768. Under review for the 28th Int. Conference on Offshore Mechanics and Arctic Engineering , Honolulu, Hawaii.